Centripetal molecules as multifunctional building blocks for coordination networks†

Yan-Qiong Sun,[a] Jun He,[a] Zhengtao Xu,*[a] Guo Huang,[a] Xiao-Ping Zhou,[a] Matthias Zeller[b] and Allen D. Hunter[b]

Received (in Cambridge, UK) 2nd July 2007, Accepted 31st August 2007
First published as an Advance Article on the web 10th September 2007
DOI: 10.1039/b709942h

Centripetally shaped molecules are crystallized with $AgSbF_6$ to yield coordination networks featuring novel coordination modes, network connectivity and chiral/helical structures.

The development of functional organic ligands constitutes an essentially important exercise in the field of coordination networks (or metal–organic frameworks),[1] as one major advantage of these networks hinges upon the much richer chemical functionalities in comparison to the inorganic crystalline materials. Particularly attractive are systems of building blocks that provide for convenient and systematic functional modifications in both molecular and solid state structure.[2] Most reported metal–organic frameworks, however, are based on relatively simple organic ligands—additional functional groups therefore tend to substantially alter the coordinating characteristics, and consequently complicate the control of the solid state structure.

We here introduce a class of branchy molecules with back-folded, centripetal geometry as functional building blocks for coordination networks. A relatively simple system is shown in Chart 1. Therein, a diacetylene-based linear rod forms the main branch (*i.e.*, G1 branch, G standing for generation), and the corresponding two terminal sites (G1 sites) are equipped with the cyano group. From the G1 branch outgrow four phenylacetylene side chains (*i.e.*, the G2 branches) terminated by the methoxy groups.

A number of advantages can be readily identified from these molecules. Thus the spatially well-removed G1 and G2 sites can be modified systematically without compromising the coordinating ability of each other. For example, the methoxy groups in **L1** can be replaced by the thiomethoxy group to probe the impact on the formation of the coordination network. In addition, the centripetal shape provides for the G2 branches to restrict the rotation of the diacetylene unit of the G1 branch, and thus creating a potentially chiral molecular scaffold similar to the atropisomers in general organic chemistry. As will be shown in this paper, the conformation can be captured in an enantiomeric form in the crystal structure, lending potential use to the construction of noncentrosymmetric solid state materials. Also, the centripetal orientation of the G2 sites of thiomethoxy composes an inchoate spiral shape, and is thus primed to be interlinked by metal ions to generate potentially interesting topological and helical features in the resultant network.

Even though molecules with rigid back-bended side chains reminiscent of the above centripetal geometry have been reported,[3] the purposeful integration of the centripetal geometry into crystalline networks appears to be unprecedented. As a preliminary exploration in this direction, we here report two crystal structures based on Ag(I) salt and the above **L1** and **L2** ligands. In particular, we wish to highlight how the modification of the G2 sites impacts the network formation, and the potential noncentrosymmetric and helical features in the solid state.

The complex $2\mathbf{L1}\cdot4AgSbF_6\cdot8C_6H_6$ (**1**) was obtained from reacting a toluene solution of $AgSbF_6$ with a benzene solution of **L1**, and the complex $\mathbf{L2}\cdot AgSbF_6$ (**2**) from the toluene solution of $AgSbF_6$ with a THF solution of **L2**.‡ X-Ray single-crystal analysis§ reveals that complex **1** crystallizes in the noncentrosymmetric space group $P3_121$ and consists of 1D coordination chains based on the linear coordination of the –CN groups to the Ag(I) ions (Fig. 1) The **L1** molecules all adopt similar conformations with a C_2 symmetry, and display the same atropisomeric chirality (Fig. S4, ESI†). Overall homochiral features are thus preserved in the coordination chains and throughout the crystal structure.

The coordination chains are aligned in a parallel fashion to form a distinct layer perpendicular to the *c* axis. The layers are packed such that the coordination chains are successively rotated by 60° in the same direction proceeding across the neighboring layers along the *c* axis (Fig. 2). The packing thus creates equilateral, triangular channels along the *c* axis, which are filled with a second set of Ag(I) ions bound by three benzene molecules (the $Ag^+\cdot3C_6H_6$ complex) and the SbF_6^- anions (see Fig. 1, S5 and S6, ESI† for the complete coordination environments of the three distinct Ag ions). The $Ag^+\cdot3C_6H_6$ complex here represents an entrapped version of the previously reported complex $AgBF_4\cdot3C_6H_6$,[4] and features a

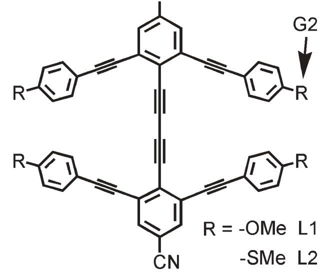

Chart 1

---

[a] *Department of Biology and Chemistry, City University of Hong Kong, 83 Tat Chee Avenue, Kowloon, Hong Kong, P. R. China. E-mail: zhengtao@cityu.edu.hk; Fax: +852-27844679*
[b] *Department of Chemistry, Youngstown State University, One University Plaza, Youngstown, Ohio, 44555, USA*
† Electronic supplementary information (ESI) available: Experimental section, additional crystallography figures and spectra, and further crystallographic data. See DOI: 10.1039/b709942h

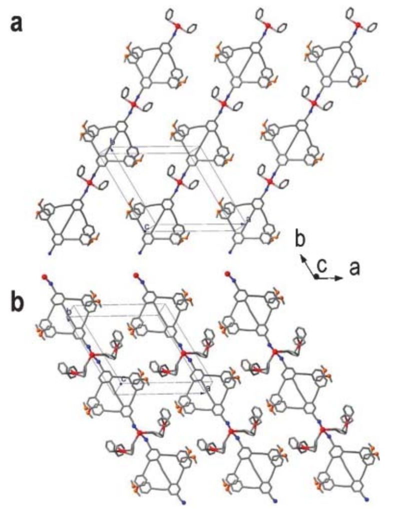

Fig. 1 Parallel alignments of the coordination chains in **1**: (a) chains of Ag1 ions; (b) chains of Ag2 ions. Red spheres, Ag; blue, N; orange, O; grey, C.

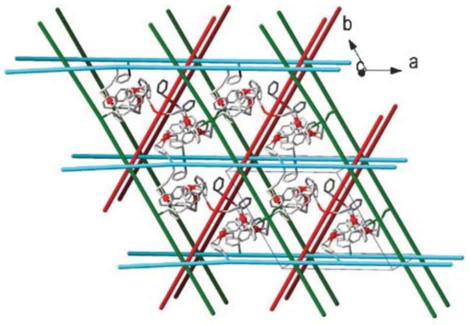

Fig. 2 Schematic presentation of the packing arrangement for the coordination chains (shown as individual rods) of **1**. The $Ag^+{\cdot}3C_6H_6$ complexes in the channels are also shown.

rare case of a discrete complex included in a coordination host network.

The packing motif of the coordination chains as described above suggests a 6_1 screw element along the *c* axis. The actual 3_1 symmetry in the crystal structure is due to the two crystallographically inequivalent layers that alternate with each other along the *c* axis. Specifically, one layer contains the Ag1 ions in the constituent coordination chains, while the other contains Ag2. The Ag1 ion is coordinated to two crystallographically related benzene molecules that are incorporated as guest molecules (Fig. S5, ESI†), while Ag2 is bonded to two of the above-mentioned $Ag^+{\cdot}3C_6H_6$ complexes *via* one of the three benzene molecules (Fig. S6, ESI†). Although the Ag atoms and the benzene guests are disordered over two sets of positions, the shorter Ag···C distances can be deduced as being about 2.40 Å and above, which compares well with the Ag···C distances in other arene–Ag(I) complexes.[5,6]

The structure of **2** was refined in the noncentrosymmetric space group $I\bar{4}2d$, with one half **L2** molecule and one $AgSbF_6$ unit contained in the asymmetric portion of the unit cell. Like in **1**, the cyano groups of the **L2** ligands coordinate to the Ag(I) ions in a linear fashion to establish a chain of alternating **L2** molecules and Ag(I) ions [Ag–N distances: 2.244(4) and 2.274(5) Å], with the **L2** ligands adopting the same chiral atropisomeric configuration throughout the crystal structure (Fig. 3). However, unlike the free-standing methoxy groups in **1**, the thiomethoxy (MeS–) groups on the crossing G2 branches of **L2** provide additional coordination bonds to the Ag(I) centers [Ag–S distances: 2.378(5)–2.582(2) Å], and bridge the parallel-aligned chains into a 2D coordination network (Fig. 3). Thus the Ag(I) ion interacts with two pairs of sulfur atoms at notably different distances (the S atoms from one pair are both at 2.378 Å and the other at 2.702 Å), forming a highly distorted octahedral geometry together with the two –CN groups. Note also that each pair of S atoms emanate from the same molecule which thus chelates the Ag(I) center in a macrocylic, tweezer-like motif encompassing two crossing side arms (G2 branches) and the diacetylene backbone (Fig. S4, ESI†).

The tweezer-like chelation motif take on an inchoate spiral shape, and, as a result, two types of double-stranded helix structures can be identified within the 2D coordination layer (Fig. 3). The first type runs perpendicular to the Ag–CN coordination chain (along the *b* axis). The constituent strand therein follows two *meta*-positioned phenylacetylene (G2) side arms and the associated Ag(I) ions as the repeating unit, with each complete turn involving four side arms (from two **L2** molecules) and two Ag(I) ions [pitch: 42.8084(8) Å (Fig. 3(a), S8, ESI†)]. The two strands are of the same chirality (*e.g.*, both right-handed in the structure of Fig. 3), and they intersect periodically at the Ag(I) ions, and are interlinked by the diacetylene units of the **L2** molecules involved.

The second type of double-stranded helix runs parallel to the Ag–CN coordination chains, and occupies the space between every two neighboring Ag–CN coordination chains (Fig. 4). The repeating unit consists of one benzonitrile group, one of its two G2 side arms, and the associated Ag(I) center. Each complete turn contains two such repeating units, with a pitch of 21.4042(8) Å (Fig. 3(c), S9, ESI†). The benzonitrile groups point in the same direction within each single strand, and thus create a net overall dipole. The polarities of the two strands are, however, opposite, resulting in no net polarization for the double helix (reminiscent of the opposing directions of the two strands in the DNA double

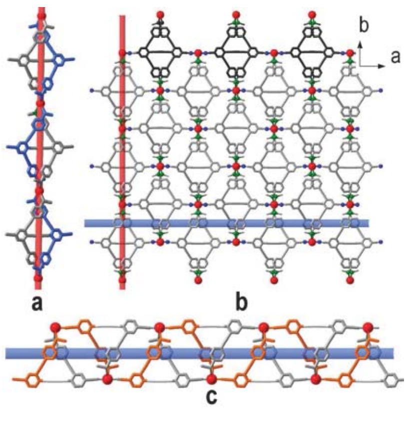

Fig. 3 (a) The double-stranded helix structure along the *b* axis in **2**. The blue and grey colors highlight the two individual strands. (b) The 2D coordination network of **2**. A linear Ag–CN chain is marked black on top for clarity. Color code: Ag, red; S, green; C, grey; N, blue. (c) The tubular structure based on two helical strands (marked orange and grey, respectively) along the *a* axis.

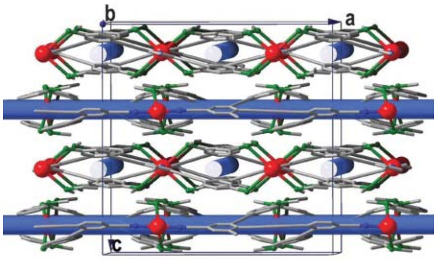

Fig. 4 Packing of the 2D coordination nets in **2**, highlighting the perpendicular orientation of the neighboring nets. Color code: Ag, red; S, green; C, grey; N, blue.

helix). The two strands intersect at the Ag(I) centers, and are chemically linked through the diacetylene units between the benzonitrile groups (note that the two crossing G2 arms from the **L2** molecule in Fig. 3(c) belong to the two different strands). Unlike the first type of helix, where the intersecting Ag(I) ions and the interlinking diacetylene units are located around the center of the helix, the Ag(I) ions and the diacetylene units are located along the wall region of the helix, thus imparting a tubular feature to the helix. The end-on view reveals a rather squashed shape of the tubes, mainly due to the flattened conformation of the constituent **L2** molecules. No space is thus available for inclusion of counterions or guests.

The solid sample of **1** is unstable in air, and quickly loses the benzene guests and decomposes into an amorphous black solid. TG analysis of an as-synthesized solid sample of **1** was able to capture part of the initial step of weight loss of 4.46% at around 100 °C (Fig. S3, ESI†), which corresponds to the removal of two benzene molecules per formula unit (calc. 4.41%). The sample instability was also reflected in a series of fluorescence spectra taken over time, which featured steady decrease of the emission intensity (Fig. S10, ESI†).

Fluorescence measurements of **L1** and **L2** show that the overall emission features in THF ($\lambda_{\text{max-}\mathbf{L1}}$ = 492 nm, $\lambda_{\text{max-}\mathbf{L2}}$ = 540 nm) are similar to those in the solid state ($\lambda_{\text{max-}\mathbf{L1}}$ = 500 nm, $\lambda_{\text{max-}\mathbf{L2}}$ = 532 nm), although the respective reasons for the red shift in the **L1** case (*i.e.*, from 492 to 500 nm) and the blue shift for **L2** (from 540 to 532 nm) are unclear at this point. By comparison, the emission peaks of complexes **1** and **2** both shift, in a larger degree, to the red ($\lambda_{\text{max-}\mathbf{1}}$ = 546 nm, $\lambda_{\text{max-}\mathbf{2}}$ = 565 nm, Fig. S11 and S12, ESI†). Theoretical study of the electronic structures of the ground and excited states of these centripetal molecules might help account for the impact of the Ag(I) species on the fluorescence properties.

In a wider perspective, the centripetal shape can be installed in a more complex molecular scaffold. For example, the G1 branches can take on a trigonal or tetragonal shape, as shown in molecules **M1** and **M2** in the ESI.† Or, one can equip the G2 branches with G3 branches in a similarly centripetal form (see **M3** in ESI†), and thus begin to approach a structural hierarchy comparable to that of dendrimers. The syntheses of these novel self-similar molecules are underway, and their use in constructing functional coordination networks and other supramolecular aggregates will be explored in due course.

This work is supported by a grant from the Research Grants Council of the Hong Kong Special Administrative Region, China [Project No. 9041109 (CityU 102406)]. Y. S. is supported by a postdoctoral grant from the Research Scholarship Enhancement Scheme of City University of Hong Kong. The diffractometer was funded by NSF grant 0087210, by the Ohio Board of Regents grant CAP-491, and by YSU.

Notes and references

‡ *Syntheses* of **1** and **2**: A benzene solution of **L1** (2.3 mg, 3.0 mM, 0.5 mL) or a THF solution of **L2** (2.6 mg, 3.0 mM, 0.5 mL) was loaded into a glass tube and carefully layered with a toluene solution of $AgSbF_6$ (2.4 mg, 7.0 mM, 0.5 mL) without disturbing the interface. The tube was then sealed and kept in the dark. Needle-like, yellow crystals of **1** and orange diamond crystals of **2** suitable for X-ray studies were obtained after one week. Yield: 83 and 34% for **1** and **2** (based on **L1** or **L2**, respectively). Chemical analysis of **1** yields the following: found: C 52.01, H 3.04, N 1.76%. This result closely matches the formula $C_{150}H_{106}Ag_4F_{24}N_4O_8Sb_4$ (*i.e.*, $2\mathbf{L1}\cdot4AgSbF_6\cdot7C_6H_6$): calc.: C 51.97, H 3.08, N 1.62%, suggesting partial loss of the benzene molecules during the sample preparation and measurement process. For comparison, formula $C_{156}H_{112}Ag_4F_{24}N_4O_8Sb_4$ (*i.e.*, $2\mathbf{L1}\cdot4AgSbF_6\cdot8C_6H_6$) gives the following calculated composition: C 52.85, H 3.18, N 1.58%. Anal. Calc. for $C_{54}H_{32}AgF_6N_2S_4Sb$ **2**: C 54.93, H 2.73, N 2.37. Found: C 54.00, H 3.26, N 2.88%.

§ *Crystal data* for **1**: $C_{156}H_{112}Ag_4F_{24}N_4O_8Sb_4$, M_r = 3545.02, trigonal, space group $P3_121$, $a = b$ = 21.368(1), c = 27.279(3) Å, V = 10786(1) Å^3, Z = 3, D_c = 1.637 g cm^{-3}, μ = 1.362 mm^{-1}, F(000) = 5244, GOF = 1.233, A total of 92898 reflections were collected and 14532 are unique (R_{int} = 0.0395). $R1$ ($wR2$) = 0.0654 (0.1626) for 1071 parameters and 14532 reflections [$I > 2\sigma(I)$]. For **2**: $C_{54}H_{32}AgF_6N_2S_4Sb$, M_r = 1180.68, tetragonal, space group $I\bar{4}2d$, $a = b$ = 21.4042(8), c = 21.408(2) Å, V = 9807.9(9) Å^3, Z = 8, D_c = 1.599 g cm^{-3}, μ = 1.182 mm^{-1}, F(000) = 4688, GOF = 1.065. A total of 36308 reflections were collected and 6110 are unique (R_{int} = 0.0605). $R1$ ($wR2$) = 0.0497 (0.1116) for 330 parameters and 6110 reflections [$I > 2\sigma(I)$]. The intensity data were collected on a Bruker AXS SMART APEX CCD diffractometer with graphite-monochromated Mo-Kα radiation (λ = 0.71073 Å) at 100 K. All absorption corrections were performed using the SADABS program. The structures were solved by direct methods and refined by full-matrix least squares on F^2 using the SHELXTL 6.14 program package. CCDC 646836 (**1**) and 646837 (**2**). For crystallographic data in CIF or other electronic format see DOI: 10.1039/b709942h

1 (*a*) C. Janiak, *Dalton Trans.*, 2003, 2781; (*b*) S. L. James, *Chem. Soc. Rev.*, 2003, **32**, 276; (*c*) B. Kesanli and W. Lin, *Coord. Chem. Rev.*, 2003, **246**, 305; (*d*) S. R. Batten and R. Robson, *Angew. Chem., Int. Ed.*, 1998, **37**, 1461; (*e*) N. W. Ockwig, O. Delgado-Friedrichs, M. O'Keeffe and O. M. Yaghi, *Acc. Chem. Res.*, 2005, **38**, 176.

2 (*a*) Z. Xu, Y.-H. Kiang, S. Lee, E. B. Lobkovsky and N. Emmott, *J. Am. Chem. Soc.*, 2000, **122**, 8376; (*b*) C.-D. Wu, A. Hu, L. Zhang and W. Lin, *J. Am. Chem. Soc.*, 2005, **127**, 8940; (*c*) Y. Cui, S. J. Lee and W. Lin, *J. Am. Chem. Soc.*, 2003, **125**, 6014; (*d*) J. D. Wuest, *Chem. Commun.*, 2005, 5830.

3 (*a*) C. R. Woods, M. Benaglia, S. Toyota, K. Hardcastle and J. S. Siegel, *Angew. Chem., Int. Ed.*, 2001, **40**, 749; (*b*) R. Nandy, M. Subramoni, B. Varghese and S. Sankararaman, *J. Org. Chem.*, 2007, **72**, 938; (*c*) V. Narayanan, S. Sankararaman and H. Hopf, *Eur. J. Org. Chem.*, 2005, 2740; (*d*) J. A. Marsden, M. J. O'Connor and M. M. Haley, *Org. Lett.*, 2004, **6**, 2385; (*e*) J. D. Bradshaw, L. Guo, C. A. Tessier and W. J. Youngs, *Organometallics*, 1996, **15**, 2582; (*f*) M. Laskoski, W. Steffen, J. G. M. Morton, M. D. Smith and U. H. F. Bunz, *J. Organomet. Chem.*, 2003, **673**, 25.

4 A. S. Batsanov, S. P. Crabtree, J. A. K. Howard, C. W. Lehmann and M. Kilner, *J. Organomet. Chem.*, 1998, **550**, 59.

5 M. Munakata, L. P. Wu, T. Kuroda-Sowa, M. Maekawa, Y. Suenaga, G. L. Ning and T. Kojima, *J. Am. Chem. Soc.*, 1998, **120**, 8610.

6 E. L. Elliott, G. A. Hernandez, A. Linden and J. S. Siegel, *Org. Biomol. Chem.*, 2005, **3**, 407.